


Research

Identification of differentially expressed MiRNA clusters in cervical cancer

S. Sriharikrishnaa¹ · Padacherri Vethil Jishnu¹ · Vinay Koshy Varghese¹ · Vaibhav Shukla¹ · Sandeep Mallya² · Sanjiban Chakrabarty^{1,3} · Krishna Sharan⁴ · Deeksha Pandey⁵ · Shama Prasada Kabekkodu^{1,3} 

Received: 31 July 2024 / Accepted: 6 February 2025

Published online: 13 February 2025

© The Author(s) 2025 

Abstract

Background Aberrant miRNA expression has been associated with cervical cancer (CC) progression. The present study aimed to identify the miRNA clusters (MCs) altered in CC, identify their clinical utility, and understand their biological functions via computational analysis.

Methods We used small RNA sequencing and qRT–PCR to identify and validate abnormally expressed MCs in cervical squamous cell carcinoma (CSCC) samples. We compared our data with publicly available CC datasets to identify the differentially expressed MCs in CC. The potential targets, pathways, biological functions, and clinical utility of abnormally expressed MCs were predicted via several computational tools.

Results Small RNA sequencing revealed that 229 miRNAs belonging to 48 MCs were significantly differentially expressed in CSCC (p-value ≤ 0.05). Validation by qRT–PCR confirmed the downregulation of members of the miR-379/656, namely, hsa-miR-376c-3p (2.8-fold; p-value 0.03), hsa-miR-494-3p (3.4-fold; p-value 0.02), hsa-miR-495-3p (eightfold; p-value 0.01), and hsa-miR-409-3p (fivefold; p-value 0.03), in CSCC samples compared with normal samples. The prognostic model generated via miRNA expression and random forest analysis showed robust sensitivity and specificity (0.88 to 0.92) in predicting overall survival. In addition, we report 22 prognostically important miRNAs in CC. Pathway analysis revealed the enrichment of several cancer-related pathways, notably p53, the cell cycle, viral infection and MAPK signalling. *CDC25A*, *CCNE1*, *E2F1*, *CCNE2*, *RBL1*, *E2F3*, *CDK2*, *RBL2*, *E2F2* and *CCND2* were identified as the top ten gene targets of MC. Drug–gene interaction analysis revealed enrichment of 548 approved drugs and 62 unique genes.

Conclusion Our study identified MCs, their target genes, their prognostic utility, and their potential functions in CC and recommended their usefulness in CC management.

Keywords MiRNA cluster · Cervical cancer · GEO · Bioinformatics · Drug–gene interaction · Gene Ontology

Supplementary Information The online version contains supplementary material available at <https://doi.org/10.1007/s12672-025-01946-0>.

✉ Shama Prasada Kabekkodu, shama.prasada@manipal.edu; spbhat81@gmail.com | ¹Department of Cell and Molecular Biology, Manipal School of Life Sciences, Manipal Academy of Higher Education, Manipal, Karnataka 576104, India. ²Department of Bioinformatics, Manipal School of Life Sciences, Manipal Academy of Higher Education, Manipal, Karnataka, India. ³Center for DNA Repair and Genome Stability (CDRGS), Manipal Academy of Higher Education, Manipal, Karnataka, India. ⁴Department of Radiotherapy Oncology, Kasturba Medical College, Manipal, Karnataka, India. ⁵Department of Obstetrics and Gynecology, Kasturba Medical College, Manipal, Karnataka, India.



1 Introduction

Cervical cancer (CC) was responsible for approximately 604,000 new cases and 342,000 deaths in 2020 [1]. (Epi) genetic abnormalities and infection with high-risk human papillomavirus (hr-HPV) are the key risk factors for CC. Overall, China and India account for more than one-third of all CC cases worldwide [2]. The global age-standardized incidence (ASI) and mortality (ASM) rates for CC are approximately 13.1 and 6.9 per 100,000 women, respectively [3]. However, the ASI rates and ASM rates in India due to CC are 14.7 and 9.2 per 100,000 women, respectively. For localized, regional, and distant diseases, the 5-year overall survival rates are 92%, 58%, and 18%, respectively [3]. Hence, there is a need to understand CC at the molecular level [4].

Pap smear analysis, HPV typing and visual inspection with acetic acid are routinely used for screening CC [5]. Some studies have recommended the use of squamous cell carcinoma antigen (SCC-Ag), cancer antigen 125 (CA-125), carcinoembryonic antigen (CEA), cancer antigen 19-9 (CA 19-9), and cytokeratin 19 fragment antigen 21-1 (CYFRA 21-1) for CC screening in clinical settings [6]. Unfortunately, these techniques have either poor specificity or sensitivity. For example, the Pap test may yield false-negative results and is reported to have low sensitivity [7]. Furthermore, testing positive for HPV does not indicate CC, and 20% of patients screened solely with HPV testing are misdiagnosed [8]. The combined use of HPV and Pap testing has been reported to improve the sensitivity and specificity for detecting CC [9]. Thus, molecular analysis may help overcome the problems associated with current CC screening methods by providing more sensitive biomarkers.

Genome-wide studies have revealed that genomic and epigenomic changes may be responsible for tumorigenesis [10]. Validation and functional analyses of the findings from genome-wide studies have revealed the utility of molecular changes as diagnostic and prognostic markers for CC [11]. It is now well accepted that microRNAs (miRNAs) are critical for regulating gene expression. We and others have shown that miRNAs are often abnormally expressed in CC and have the potential to be used in the clinical management of CC [12]. The human genome contains miRNA groups known as miRNA clusters [13]. A miRNA cluster (i) contains two or more individual miRNA-encoding genes regulated by a single promoter or regulator unit, (ii) shows co-expression and (iii) is transcribed in the same orientation. Furthermore, the members of the miRNA cluster target the same gene or different genes belonging to the same pathway. According to miRbase, the human genome contains 159 miRNA clusters [14]. Given that miRNA clusters hosts many miRNA-encoding genes, their biological impact is anticipated to be greater than that of individual miRNAs [15]. However, the regulation, biological function, and mechanism of abnormal expression of large miRNA clusters and their contributions to tumorigenesis are poorly known.

Aberrant miRNA expression is reported during the development and progression of CC. Unfortunately, we do not know the complete set of miRNA clusters altered in CC. In this pilot study, we aimed to identify differentially expressed miRNA clusters in CC patients, construct a miRNA cluster-target gene network, and understand their biological function via an in-silico approach. In this study, we performed small RNA sequencing in freshly collected normal and cervical squamous cell carcinoma tissues (CSCC) to identify differentially expressed miRNAs. The differentially expressed miRNAs are annotated to miRNA clusters. We compared our data with The Cancer Genome Atlas (TCGA) and Gene Expression Omnibus (GEO) datasets to identify the commonly altered miRNA clusters in CC. We constructed a prognostic model using the abnormally expressed miRNA clusters, built a protein–protein interaction network of miRNA cluster target genes, and identified the hub genes. Additionally, we performed functional and pathway enrichment analyses and drug–gene interaction analyses. Overall, our study identified several known and novel miRNA clusters with potential for CC management.

2 Materials and methods

2.1 Sample collection

In the present study, 21 normal cervical epithelium (NCE) samples and 21 cervical squamous cell carcinoma (CSCC) samples were retrospectively collected. The study was approved by the Institutional Ethical Committee at Kasturba Hospital, Manipal (IEC763/2016), and conducted in accordance with the principles of the Declaration of Helsinki. Written informed consent was obtained from all participants prior to sample collection. CSCC tissues were collected

via punch biopsy. The CSCC samples with over 80% tumor cells according to histopathological examination by an experienced pathologist were included only in the study. Exfoliative cytology samples collected via a cytobrush from healthy women undergoing routine cervical examination at Kasturba Medical College, Manipal, were used as NCEs. The NCE samples included in the study were age-matched with no previous history of any cancer. Newly diagnosed and freshly operated cervical tissue samples were collected in sterile vials. The study excluded patients who had received any pre-surgery treatment [12]. Samples were collected between December 2016 and December 2021 from the Departments of Radiotherapy and Oncology and Obstetrics and Gynaecology at Kasturba Medical College, Manipal, India.

2.2 Nucleic acid extraction

We isolated DNA and total RNA via the Genomic DNA Purification Kit (HiMedia, India) and mirVana Total RNA isolation Kit (Thermo Fisher Scientific, USA). The extracted DNA and RNA were stored at -20°C and -80°C [12]. We evaluated the quality and quantity of the DNA via agarose gel electrophoresis and a Nanodrop spectrophotometer (Thermo Fisher Scientific, USA). We assessed the quantity of total RNA via a Qubit fluorometer (Thermo Fisher Scientific, USA). We used an RNA-6000 nanochip and Bioanalyzer machine (Agilent Technologies, USA) to test the quality and integrity of the RNA. Samples with an RNA integrity number (RIN) > 7 were taken for small RNA sequencing as published earlier [12].

2.3 HPV testing

We conducted nested PCR using PGMY09/PGMY11 and GP5⁺/GP6⁺ to detect the presence of HPV in the samples. A PCR showing a 450 bp band for PGMY09/PGMY11 primers and a 150 bp band for GP5⁺/GP6⁺ were considered positive for HPV. The PCRs included 100 ng of DNA, 200 nM each primer, 100 nM dNTPs, 1 U/ μL Taq DNA polymerase, and PCR buffer containing 2.5 mM MgCl_2 . The primers and PCR cycles used were described previously [16]. We used PCR for the beta-globin gene as an internal control. DNA from a cervical cancer cell line (SiHa) served as a positive control.

2.4 Small RNA sequencing

Total RNA isolated from NCE and CSCC ($n = 11$ each) was sequenced according to our previously published small RNA sequencing workflow [12]. Briefly, small RNAs were enriched from total RNA via a Total RNA-Seq Kit v2. The quality and quantity of the enriched small RNAs were measured via an Agilent® small RNA kit in a 2100 Bioanalyzer instrument (Agilent Technologies, USA). After barcoding via the Ion Xpress™ RNA-Seq Barcode 1–16 Kit, the samples were sequenced by generating sequencing templates via the Ion OneTouch™ 2 system and Ion OneTouch™ ES. We used a P1™ chip and Ion Proton system™ (Thermo Fisher Scientific, USA) for sequencing. Small RNA sequencing was performed without duplicate samples. All sequencing reagents were procured from Thermo Fisher Scientific, USA [12].

2.5 MiRNA data analysis

Torrent Suite™ software was initially used to process the raw data. Preprocessing, alignment, and identification of differentially expressed miRNAs were carried out via the CAP-miRSeq pipeline [17]. We used the DESeq2 package in R and applied a false discovery rate (FDR) correction to adjust for multiple comparisons. We considered miRNAs to be differentially expressed if LogFC (log_2 fold change) $> +1$ and < -1 with an FDR threshold of 0.05, $p < 0.05$ and a minimum average number of reads of 20. We used the Benjamini–Hochberg false discovery rate (FDR) with a 5% alpha level for raw p-value correction. This threshold ensures that the control over the expected proportion of false positives is less than 5%. This FDR correction was applied to account for multiple testing and enhance the robustness of our findings by identifying differentially expressed miRNA clusters.

2.6 Identification of miRNA clusters

MiRNA counts were first normalized, log_2 -transformed, and then assigned to the miRNA cluster by comparing the individual differentially expressed miRNAs with those in the MetaMirClust database. MetaMirClust is a comprehensive database containing miRNA clusters in the human genome and their annotations [18]. We downloaded the list of miRNAs belonging to the miRNA cluster from the MetaMirClust database. Differentially expressed miRNAs identified from small

RNA sequencing and miRNAs belonging to miRNA clusters were exported to Microsoft Excel. The common miRNAs identified via the VLOOKUP function in Microsoft Excel were considered differentially expressed miRNA clusters.

2.7 qRT–PCR

We performed TaqMan based qRT–PCR via 7500 Fast real-time PCR (Thermo Fisher Scientific, USA) to validate the NGS findings. TaqMan assay probes and reagents were purchased from Thermo Fisher Scientific, USA. We selected TaqMan assay probes hsa-miR-376c-3p (Assay ID 002122), hsa-miR-494-3p (Assay ID 002365), hsa-miR-495-3p (Assay ID 001663), and hsa-miR-409-3p (Assay ID 002332) for validation of the NGS data in an independent cohort of NCE and CESC samples ($n = 10$ each). We used 10 ng/ μ L total RNA and the TaqMan® MicroRNA Reverse Transcription Kit (Thermo Fisher Scientific, USA) to carry out reverse transcription. RNU6B (ID 001093) served as an internal control for qRT–PCR. Differential miRNA expression was quantified via the $2^{-\Delta\text{Ct}}$ formula, where $\Delta\text{Ct} = \text{Ct value of test miRNA} - \text{Ct value of RNU6B}$ [11, 12].

2.8 MiRNA cluster target identification

miRNA cluster targets were predicted via the miRTarBase (V8.0) [19], TargetScan (V8.0) [20], and miRDIP (V5.2) [21] databases with the default settings. The targets commonly predicted by all three databases were considered putative targets. We next analysed the expression of miRNA cluster target genes in the TCGA-CESC datasets. The genes that showed differential expression in the TCGA-CESC dataset and an inverse correlation with clustered miRNAs were used for all downstream analyses.

2.9 Interaction, functional, and pathway enrichment analysis

We used the ShinyGO (V0.80) web server to predict the gene ontology (GO) terms and pathways enriched in response to abnormal miRNA cluster expression [22]. A protein–protein interaction network (PPIN) of miRNA cluster targets was constructed via STRING (V12.0) [23] with the default parameters. From the PPIN, the top ten hub genes (HGs) were identified via the cytoHubba tool [24], and their interactions were visualized via Cytoscape (V3.10.2) [25].

2.10 Prognostic model construction and survival analysis

We used the TACCO online tool to evaluate the prognostic significance of differentially expressed miRNAs from miRNA clusters [26]. We uploaded the differentially expressed miRNAs to the TACCO webserver and used the random forest algorithm to assess their ability to predict overall survival. The patients were categorized into high-risk and low-risk categories on the basis of the median survival in days. The signature miRNAs used to predict the high-risk and low-risk categories were selected by the Wilcoxon rank-sum test with a p -value < 0.05 . Predictive models were constructed via the random forest algorithm. We subsequently used Kaplan–Meier (KM) survival plots and log-rank tests to assess the associations between differentially expressed miRNAs and overall survival. A p -value < 0.05 was considered statistically significant.

2.11 Drug–gene interaction analysis

PanDrugs (V2.0) is a bioinformatics pipeline that can be used to prioritize anticancer agents on the basis of genome-wide OMICS studies [27]. It contains multi-OMICS data from 23 cancers and contains 74,087 drug–target interactions generated from 4642 genes and 14,659 chemical compounds. We queried the PanDrugs (V2.0) for the hub genes to identify the druggable hub genes with those of potential drugs that are under clinical trials or already approved by the FDA.

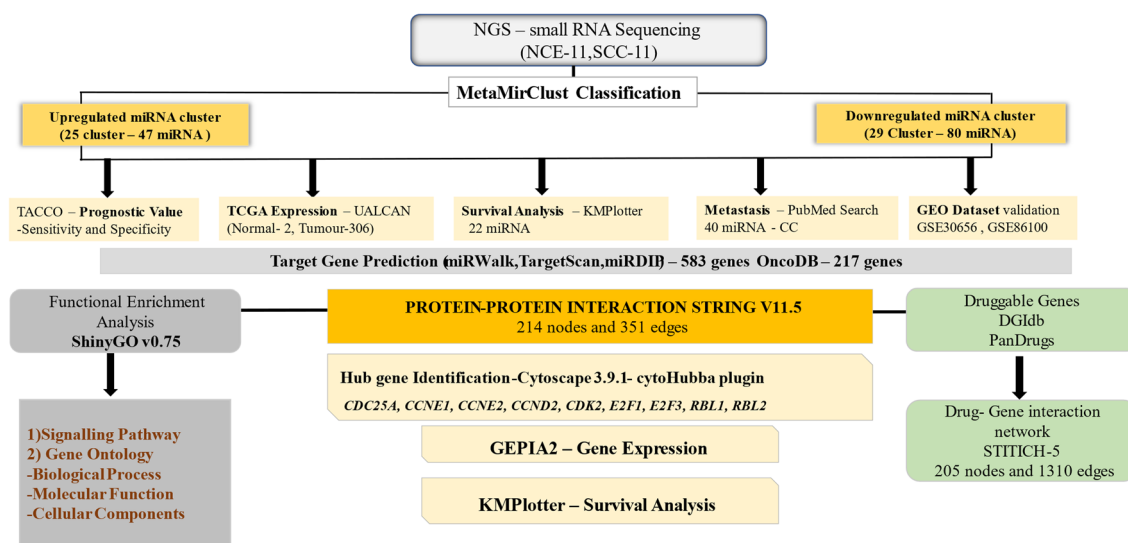
3 Results

3.1 Clinical characteristics of the patients

A total of 42 samples were analysed to identify changes in miRNA expression between CESC and NCE samples. Among these samples, 11 samples each from NCE and CESC were subjected to small RNA sequencing, while 10 samples each from NCE and CESC were used for validation through qRT–PCR. The median ages of the patients in the NCE and CESC

Table 1 Clinicopathological features of NCE and CSCC samples

Features	NCE (n = 21)	CSCC (n = 21)
Age (in years)	53 ± 9.4	57 ± 6.1
Age of menarche (in years)	14.7 ± 2.2	15.1 ± 2.9
HPV status		
Positive	0	21
Negative	21	0
Deliveries		
0–1	14	5
≥ 2	7	16
Family history of cancer		
Yes	2	10
No	11	6
Not known	8	5
FIGUREO status		
I/II	–	14
III/IV	–	7
Tumour size		
< 4 cm	–	10
≥ 4 cm	–	11
Lymph node metastasis		
Yes	–	12
No	–	9

**Fig. 1** Pictorial representation of the approach used for in silico analysis

groups were 53 and 57 years, respectively. All CSCC samples were confirmed to contain more than 80% tumor cells and were HPV positive, whereas all NCE samples were HPV negative. The clinicopathological characteristics of the samples used in the present study are shown in Table 1. Figure 1 summarizes the study outline used for in-silico identification and analysis of differentially expressed miRNA clusters, their targets, associated pathways, and drug–gene interactions.

3.2 miRNA clusters show aberrant expression in CC patients

We first compared the miRNA expression between the NCE and CSCC samples to identify the putative differentially expressed miRNAs in CC. Small RNA sequencing revealed 229 miRNAs (upregulated: 89 and downregulated: 140) that

were differentially expressed between the NCE and CSCC samples. To identify the miRNA clusters differentially expressed in CSCC samples, we extracted the human miRNA cluster genes from MetaMirClust. The comparison between MetaMirClust and our study revealed that 48 miRNA clusters were differentially expressed [22 upregulated (Fig. 2a) and 26 downregulated (Fig. 2b)] between the NCE and CSCC samples. We used the dbDEMC database to obtain differentially expressed miRNAs in cervical cancer from previously published studies. dbDEMC is a comprehensive database consisting

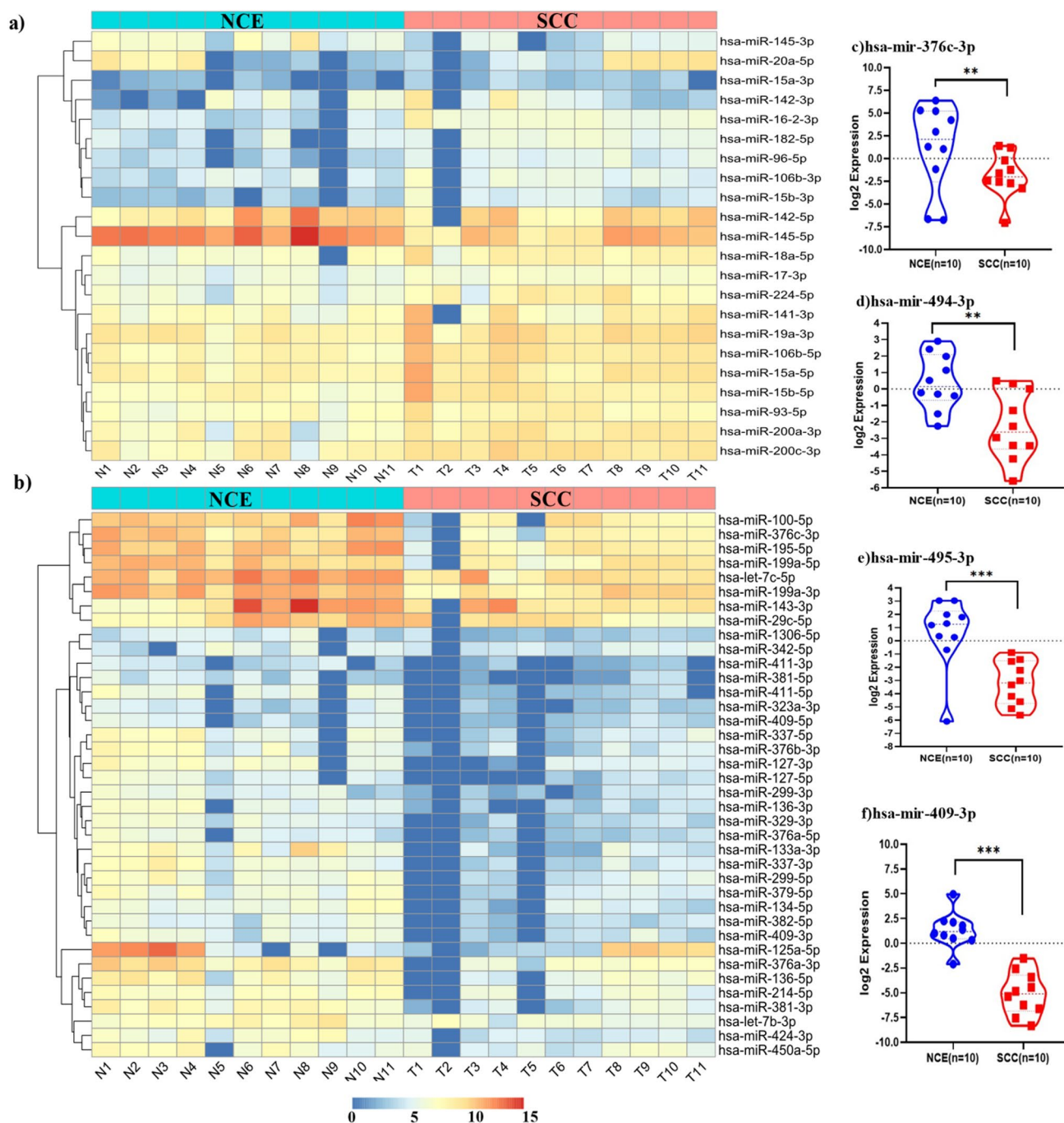


Fig. 2 Hierarchical clustering of differentially expressed miRNAs belonging to MCs between NCE and CSCC. **a** and **b** Represents significantly upregulated and downregulated miRNAs belonging to MCs in SCC as analysed by small RNA sequencing of 11 NCE and 11 CSCC samples. Validation of small RNA sequencing results via qRT-PCR in 10 NCE and 10 CSCC samples. qRT-PCR revealed significant downregulation of **c** hsa-miR-376c-3p, **d** hsa-miR-494-3p, **e** hsa-miR-495-3p, and **f** hsa-miR-409-3p in CSCC compared with NCC.RNU6B was used as an internal control. $P < 0.05$ was considered statistically significant. NCE: normal samples; CSCC: cervical squamous cell carcinoma; MCs: miRNA clusters. N1 to N11 represent 11 normal samples, and T1 to T11 represent 11 CSCC samples

of data from 403 datasets and 40 cancer types (Supplementary Fig. 1) [28]. CC gene expression datasets such as GSE30656 (10 normal and 10 tumor samples) [29], TCGA-CESC (2 normal and 307 tumor samples), and GSE86100 (6 normal and 6 tumor samples) [30] were already integrated into the dbDEMC webserver and were queried to identify the differentially expressed miRNAs. The analysis of GSE30656 identified 28 up- and 25 downregulated miRNAs. The TCGA-CESC dataset included 74 up- and 90 downregulated miRNAs. The GSE86100 dataset analysis revealed 43 up- and 30 downregulated genes. The differentially expressed miRNA data were compared with data from MetaMirClust to identify the differentially expressed miRNA cluster. The comparison revealed 16 miRNA clusters (18 upregulated and 45 downregulated) in the GSE30656 dataset, 45 miRNAs (21 upregulated and 24 downregulated) in the TCGA-CESC dataset, and 18 miRNA clusters (12 upregulated and 31 downregulated) in the GSE86100 dataset (Supplementary Table 1). The comparison between our data and the TCGA-CESC dataset identified 85 common miRNAs. These data collectively suggest that aberrant expression of miRNA clusters (Table 2) and individual miRNAs (Supplementary Table 2) occurs frequently in CC.

3.3 miR-379/656 cluster is significantly downregulated in CC

The miRNAs used for validation were shortlisted from our small RNA sequencing data. MiR-379/656 is the second largest MC in the human genome and consists of 42 miRNAs driven by a single promoter [31]. Interestingly, 31 members of the miR-379/656 cluster were downregulated according to our NGS data. However, the expression of 11 miRNAs from the cluster was undetermined according to our NGS analysis. In addition, members of this cluster were commonly downregulated in our NGS and public datasets. Hence, we selected hsa-miR-376c-3p (Fig. 2c), hsa-miR-494-3p (Fig. 2d), hsa-miR-495-3p (Fig. 2e), and hsa-miR-409-3p (Fig. 2f) miRNAs for validation in an independent cohort of normal and CESC samples (10 each) via qRT-PCR. hsa-miR-376c-3p (2.8-fold; p-value 0.03), hsa-miR-494-3p (3.4-fold; p-value 0.02), hsa-miR-495-3p (eightfold; p-value 0.01), and hsa-miR-409-3p (fivefold; p-value 0.03) were significantly downregulated in CESC samples compared with NCE samples ($p < 0.05$).

3.4 miRNA cluster can target key cancer associated signaling pathways with a potential to predict patient survival and metastasis in CC

miRNA set enrichment analysis was performed via miEAA [32]. Fifty-three KEGG pathways were significantly enriched (FDR adjusted p value < 0.01). Wnt signalling, small cell lung cancer, VEGF signalling, mTOR signalling, angiogenesis, apoptosis, EGFR signalling, and TNF- α signalling were the top enriched pathways (Supplementary Fig. 2). The volcano plot represents the significantly upregulated (Fig. 3a) and downregulated (Fig. 3b) miRNAs belonging to the miRNA clusters analysed via the TACCO webserver. We next built a prognostic model based on signature miRNAs identified via the random forest algorithm in the TACCO webserver [26]. The prognostic model generated using upregulated miRNA clusters had a sensitivity and specificity of 0.92 and 0.90, respectively (Fig. 3c). The prognostic model generated using downregulated miRNA clusters had a sensitivity and specificity of 0.88 and 0.92, respectively (Fig. 3d). Finally, we performed survival analysis for the upregulated (Fig. 3e) and downregulated (Fig. 3f) miRNAs via KM plots and log rank tests. The miRNAs used for building the prognostic model are shown in (Fig. 3g, h). A total of 15 upregulated and 7 downregulated miRNAs belonging to the miRNA cluster were identified as prognostically significant (Supplementary Table 3). Clinicopathological analysis suggested that 12 out of 21 samples (57%) presented with lymph node metastasis. We manually searched the literature to determine whether aberrant miRNA cluster expression can enhance metastatic potential. A literature search of experimental studies suggested that the upregulation of 16 miRNAs and the downregulation of 24 miRNAs may aid in metastasis in CC (Supplementary Table 3).

3.5 Aberrant miRNA cluster expression targets genes connected with cell cycle and may promote cell cycle progression

miRNA cluster targets were predicted via 3 independent target prediction tools, namely, miRTarBase (V 8.0) [20], miR-NET (V 2.0) [33], and mirDIP (V5.2) [21], which identified 583 target genes. The genes commonly predicted by the three independent databases were chosen for downstream analysis. TCGA-CESC dataset analysis via OncoDB [34] (adjusted p value: 1.00×10^{-3} , log₂FC: 1) revealed 5510 DEGs. Compared with the 5510 differentially expressed genes in the TCGA-CESC datasets, the 583 miRNA target genes identified 217 differentially expressed genes (Supplementary Table 4). The comparison between our data and the TCGA-CESC data revealed 85 common members of the miRNA cluster. We used 217 DEGs for PPIN and HG construction. The PPIN of 217 differentially expressed genes constructed using the highest

Table 2 Differentially expressed miRNA cluster and its members in CC

S.No.	miRNA clusters	Mature.ID	Expression in NGS	P value
1	miR-1/133a cluster	hsa-miR-1	- 3.689126575	0.000391660000
2		hsa-miR-133a	- 3.239382214	0.000001520000
3		hsa-miR-100	- 3.030421962	0.004260048000
4	miR-122/3591 cluster	hsa-miR-3591	- 2.61646554	0.0065544081100
5	miR-137/2682 cluster	hsa-miR-137	- 5.260708324	0.0002130000
6	miR-143/145 cluster	hsa-miR-143	- 2.892557312	0.004524228000
7		hsa-miR-145	- 2.00372615	0.000000813000
8		hsa-miR-1264	- 2.453302114	0.040312118000
9	miR-1912/1264 cluster	hsa-miR-1912	- 1.956530765	0.0178857446000
10		hsa-miR-365a	- 1.516852719	0.052876496000
11		hsa-miR-196a	- 0.956578957	0.01903431180
12	miR-199a/214 cluster	hsa-miR-199a	- 2.719920556	0.000005100000
13		hsa-miR-214	- 3.0296726	0.000125223000
14		hsa-miR-133b	- 2.000553317	0.000001520000
15	miR-206/133b cluster	hsa-miR-212	- 1.648448345	0.011426642000
16		hsa-miR-132	- 1.343608931	0.003932207000
17		hsa-miR-296	- 1.712724698	0.052333537000
18	miR-298/296 cluster	hsa-miR-29a	- 1.664212669	0.025371994000
19		hsa-miR-342	- 1.392115346	0.136509428000
20		hsa-miR-1306	- 1.961048955	0.012000596000
21	miR-212/132 cluster	hsa-miR-655	- 3.526941133	0.000317166000
22		hsa-miR-381	- 3.512721364	0.000000187000
23		hsa-miR-487b	- 3.34895716	0.000179098000
24	miR-29a cluster	hsa-miR-154	- 3.192471525	0.000018000000
25		hsa-miR-299	- 3.131033568	0.000006600000
26		hsa-miR-654	- 3.037223129	0.000006410000
27	miR-342/151b cluster	hsa-miR-376a	- 2.962153111	0.00049115900
28		hsa-miR-376b	- 2.922663708	0.00235705800
29		hsa-miR-329	- 2.846835033	0.00069466700
30	miR-3618/1306 cluster	hsa-miR-1185-1	- 2.843235883	0.08818427700
31		hsa-miR-376c	- 2.825429917	0.00051482300
32		hsa-miR-495	- 2.817754993	0.00362405200
33	miR-29a cluster	hsa-miR-656	- 2.694527214	0.00011407000
34		hsa-miR-134	- 2.692604775	0.00182246600
35		hsa-miR-539	- 2.649274472	0.0031321119
36	miR-379/656 cluster	hsa-miR-485	- 2.575265389	0.00197778500
37		hsa-miR-1185-2	- 2.514019055	0.08818427700
38		hsa-miR-379	- 2.509921273	0.00005090000
39	miR-29a cluster	hsa-miR-758	- 2.46877805	0.008705412000
40		hsa-miR-409	- 2.383408664	0.00028909100
41		hsa-miR-487a	- 2.3013612	0.00017909800
42	miR-379/656 cluster	hsa-miR-376a-2	- 2.166274223	0.00049115900
43		hsa-miR-494	- 2.14532608	0.00074267600
44		hsa-miR-1185-1	- 2.051874898	0.08818427700
45	miR-29a cluster	hsa-miR-380	- 2.027889514	0.00874140740
46		hsa-miR-377	- 1.905221755	0.05244138900
47		hsa-miR-323a	- 1.878891262	0.00496589700
48	miR-379/656 cluster	hsa-miR-543	- 1.824423002	0.02540134700
49		hsa-miR-382	- 1.818950835	0.00029057800
50		hsa-miR-411	- 1.736256464	0.04441130200
51	miR-29a cluster	hsa-miR-369	- 1.630079406	0.00012480000

Table 2 (continued)

S.No.	miRNA clusters	Mature.ID	Expression in NGS	P value
52	miR-3910 cluster	hsa-miR-3910	– 1.960703294	0.03000897600
53	miR-3960/2861 cluster	hsa-miR-3960	– 2.361139263	0.010933514500
54	miR-423/3184 cluster	hsa-miR-423	– 1.656084748	0.028077544300
55	miR-424/450b cluster	hsa-miR-450a-2	– 3.278706353	0.04634836400
56		hsa-miR-450b	– 2.929365412	0.09857484700
57	miR-424/450b cluster	hsa-miR-424	– 2.598398537	0.00032744500
58		hsa-miR-450a	– 2.362874149	0.04634836400
59		hsa-miR-542	– 1.631271823	0.07044618300
60		hsa-miR-503	– 1.404072598	0.01173034200
61	miR-4725/365b cluster	hsa-miR-365b	– 1.516852719	0.05287649600
62	miR-489/653 cluster	hsa-miR-489	– 2.047553741	0.03099116870
63	miR-493/136 cluster	hsa-miR-433	– 3.991388891	0.00000045300
64		hsa-miR-337	– 3.632090346	0.00000430000
65		hsa-miR-432	– 3.494837875	0.0061215482164
66		hsa-miR-136	– 3.322606206	0.00008250000
67		hsa-miR-665	– 2.468541222	0.007898343333
68		hsa-miR-127	– 2.428186539	0.00526632400
69		hsa-miR-493	– 1.653840687	0.011412741800
70	miR-497/ 195 cluster	hsa-miR-497	– 2.548056656	0.00000017800
71		hsa-miR-195	– 1.876138204	0.00006660000
72	miR-99b/125 cluster	hsa-miR-125a	– 2.147805949	0.0000000104
73		hsa-let-7e	– 1.897986717	0.0261012706
74		hsa-miR-99b	– 1.74890862	0.000611863
75	miR-106/363 cluster	hsa-miR-20b	3.856484756	0.00000029300
76		hsa-miR-19b	1.494672422	0.00100568800
77		hsa-miR-363	3.922960789	0.00000076600
78		hsa-miR-18b	3.578053011	0.00000054200
79		hsa-miR-106a	3.313067527	0.00010176300
80	miR-106b/25 cluster	hsa-miR-106b	1.948333524	0.00008270000
81		hsa-miR-25	1.57114627	0.00481324600
82		hsa-miR-93	1.187553109	0.0053162970800
83	miR-1179/3529 cluster	hsa-miR-7	1.924654855	0.0060942526400
84	miR-1250/338 cluster	hsa-miR-338	1.794769063	0.0081110886800
85	miR-15a/16-1 cluster	hsa-miR-15a	2.974560862	0.00169497500
86		hsa-miR-16-2	3.388717661	0.01928757100
87	miR-15b/16-2 cluster	hsa-miR-15b	2.74657455	0.00005160000
88	miR-17/92 cluster	hsa-miR-18a	2.372920556	0.00090038600
89		hsa-miR-20a	2.185993915	0.00096446900
90		hsa-miR-92a	1.701566011	0.017500985100
91		hsa-miR-19a	1.529610582	0.00214057300
92		hsa-miR-19b-1	1.494672422	0.00482537100
93		hsa-miR-17	1.040909278	0.00554282400
94	miR-181 cluster	hsa-miR-181b	1.722827952	0.016207131400
95		hsa-miR-181a-2	1.624846656	0.0046253050000
96	miR-182/183 cluster	hsa-miR-96	2.896796113	0.00009990000
97		hsa-miR-183	2.489411009	0.03383907400
98		hsa-miR-182	2.031746189	0.03065204100
99	miR-191/425 cluster	hsa-miR-425	2.138260498	0.00286583240
100	miR-200a/429 cluster	hsa-miR-200a	1.81389971	0.02446633400
101		hsa-miR-429	1.689364246	0.06522373000
102		hsa-miR-200b	1.376302614	0.09023864000

Table 2 (continued)

S.No.	miRNA clusters	Mature.ID	Expression in NGS	P value
103	miR-200c/141 cluster	hsa-miR-141	1.704453624	0.00855629500
104		hsa-miR-200c	1.276244186	0.00612169400
105	miR-221/222 cluster	hsa-miR-222	1.334785224	0.02602073
106		hsa-miR-221	1.18298287	0.0073359507900
107	miR-301b/130b cluster	hsa-miR-130b	2.035848397	0.01643066640
108	miR-33b/6777 cluster	hsa-miR-33b	2.080321632	0.00040942500
109	miR-34 cluster	hsa-miR-34b	2.697948794	0.036892451800
110		hsa-miR-34c	2.849117111	0.05749831200
111	miR-3913 cluster	hsa-miR-3913	1.682126286	
112	miR-449 cluster	hsa-miR-449a	1.775956174	0.022131862200
113	miR-452/224 cluster	hsa-miR-224	2.530517374	0.026290762500
114	miR-4732/451a cluster	hsa-miR-144	4.358115718	0.00000061000
115		hsa-miR-451a	4.05567325	0.00000036600
116	miR-4736/142 cluster	hsa-miR-142	2.638348196	0.00729918800
117	miR-486 cluster	hsa-miR-486	5.193874562	0.00004910000

confidence level of 0.9 showed 214 nodes and 351 edges (Fig. 4a, $p < 1.0\text{e}^{-16}$). The PPIN network was further screened for HGs via cytoHubba and visualized via Cytoscape [25]. The top ten HGs identified in the present study were cell division cycle 25A (CDC25A), Cyclin E1 (CCNE1), E2F Transcription Factor 1 (E2F1), CyclinE2 (CCNE2), RB transcriptional corepressor like 1 (RBL1), E2F Transcription Factor 3 (E2F3), Cyclin Dependent Kinase 2 (CDK2), RB transcriptional corepressor like 2 (RBL2), E2F Transcription Factor 2 (E2F2), and Cyclin D2 (CCND2) (Fig. 4b). The gene ontology terms enriched for biological process (Fig. 5a), molecular function (Fig. 5b), and cellular components (Fig. 5c) are shown. The cell cycle, small lung cancer, prostate cancer, cellular senescence, p53 signalling, and microRNAs in cancer appeared to be the top enriched pathways (Fig. 5d).

3.6 Drug gene interaction analysis identified known and novel drugs that can be repurposed against CC

A search of PanDrug V 2.0 using 217 differentially expressed target genes resulted in 548 approved drugs and 62 unique druggable genes (Supplementary Table 5). The distributions of drugs that are already approved, under clinical trials, and under various stages of experimentation are shown in (Fig. 6a). The drug families that were enriched in our analysis included Bcr-Abl kinase inhibitors, receptor tyrosine kinases, serine/threonine kinases, CDK inhibitors, nonreceptor tyrosine kinases, hydrolases, and HDAC inhibitors (Fig. 6b). We next constructed a drug–gene interaction network via STITCH [35] and identified approved drugs that can be repurposed for CC treatment (Fig. 6c).

4 Discussion

CC remains a significant public health burden, particularly in underdeveloped and developing nations, where incidence and mortality rates are high despite the availability of PAP screening and HPV vaccines [2]. The increasing incidence of CC globally underscores the urgent need for improved strategies for prevention and early detection. The high mortality rates of CC are often due to late diagnosis, insufficient implementation of screening programs, and the aggressive nature of the disease [36]. Understanding the molecular mechanisms underlying CC could lead to the identification of novel biosignatures, offering new avenues for diagnosis, prognosis, and targeted therapies [37]. miRNAs, known regulators of various biological processes, play crucial roles in CC by modulating pathways that contribute to cancer development and progression when abnormally expressed [38]. Identifying and understanding the functional roles of differentially expressed miRNA clusters could provide valuable insights into CC pathogenesis and potential biomarkers for clinical applications.

We performed small RNA sequencing to identify abnormally expressed miRNA clusters in CSCC. We reported 48 significantly differentially expressed miRNA clusters in CSCC patients compared with NCE samples. Since our sample size was small, we compared our data with small RNA sequencing data from 4 different small RNA sequencing studies that

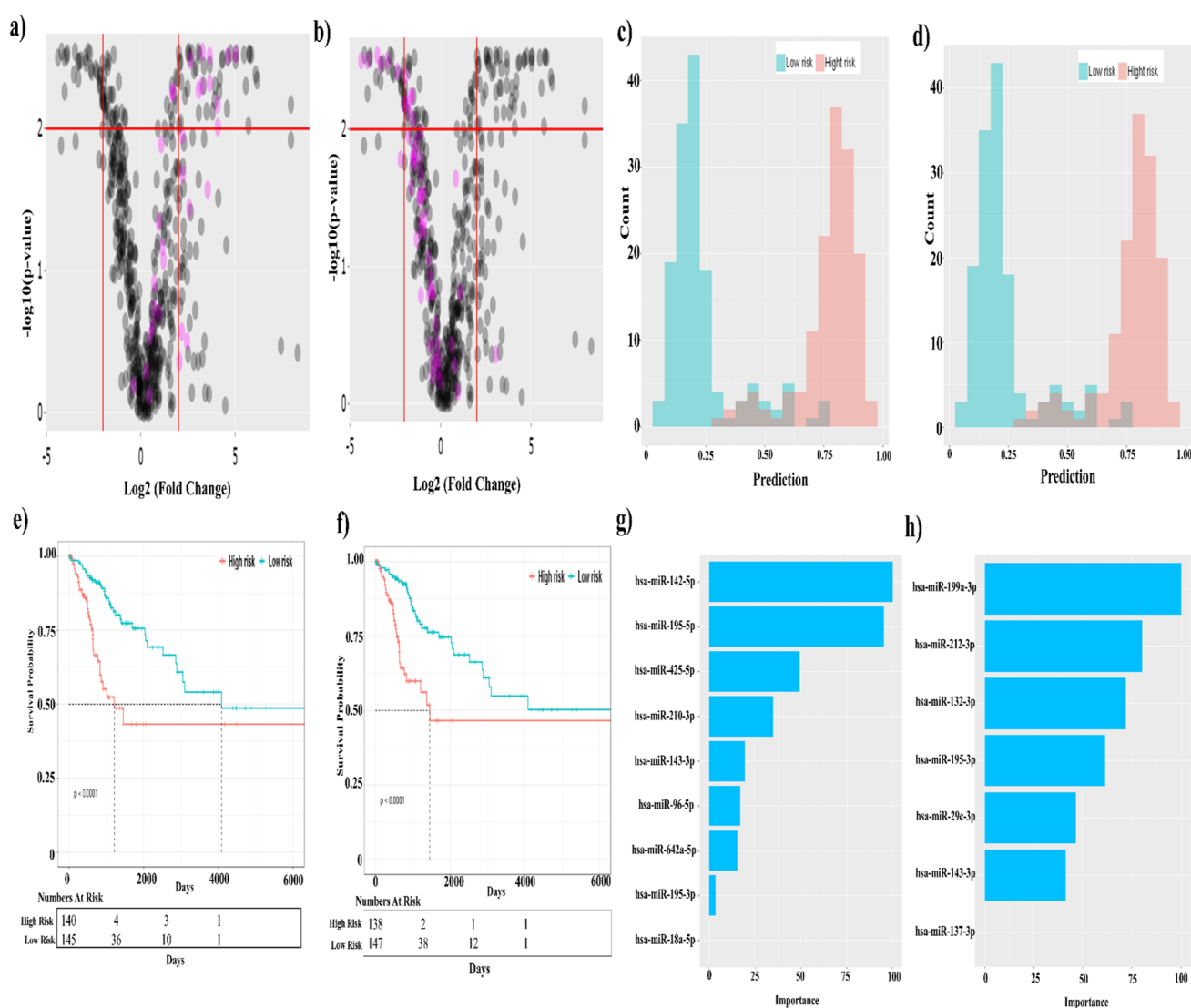


Fig. 3 MC expression can impact overall survival. We constructed a prognostic model for overall survival using upregulated and downregulated miRNAs from MCs. The random forest algorithm and TACCO webserver were used to construct the prognostic model. **a** Volcano plot of the upregulated miRNAs in the TCGA-CESC cohort. The dots coloured in pink represent the significantly upregulated miRNAs from MCs. **b** Volcano plot of the downregulated miRNAs in the TCGA-CESC cohort. The dots highlighted in pink represent the significantly downregulated miRNAs from MCs. **c** Sensitivity and specificity analysis via the random forest algorithm. The upregulated MCs had a sensitivity and specificity of 0.92 and 0.90, respectively, in differentiating the high-risk group from the low-risk group. The patients were categorized into high-risk and low-risk groups via the random forest algorithm. **d** Sensitivity and specificity analysis via the random forest algorithm. The downregulated MCs had a sensitivity and specificity of 0.88 and 0.92, respectively, to differentiate the high-risk group from the low-risk group. The patients were categorized into high-risk and low-risk groups via the random forest algorithm. **e** KM plot for overall survival predicted via upregulated MCs. The random forest algorithm was used to categorize patients into high-risk and low-risk categories on the basis of miRNA expression. High-risk and low-risk patients were tested via the log rank test, and overall survival (OS) was calculated via Kaplan–Meier (KM) survival curves. **f** KM plot for overall survival predicted via the downregulated members of MCs. The random forest algorithm was used to categorize patients into high-risk and low-risk categories on the basis of miRNA expression. High-risk and low-risk patients were tested via the log-rank test to predict overall survival. The data are represented as Kaplan–Meier (KM) survival curves. **g** The upregulated miRNAs from MCs included in the prognostic model. **h** Key downregulated miRNAs from MCs included in the prognostic model

were previously published. We next performed target gene prediction [19–21], gene ontology and pathway enrichment analyses [22] to identify the biological processes and pathways potentially regulated by the differentially expressed miRNA clusters. We noted that pathways connected to infection and cancer were highly enriched. Our study supports the findings of previous studies suggesting the strong involvement of miRNA dysregulation in the pathogenesis of CC. Furthermore, we propose that aberrant miRNA cluster expression may be a key event associated with CC. We and others suggest that aberrant miRNA expression can be used as a prognostic and therapeutic marker in CC [39]. To achieve this

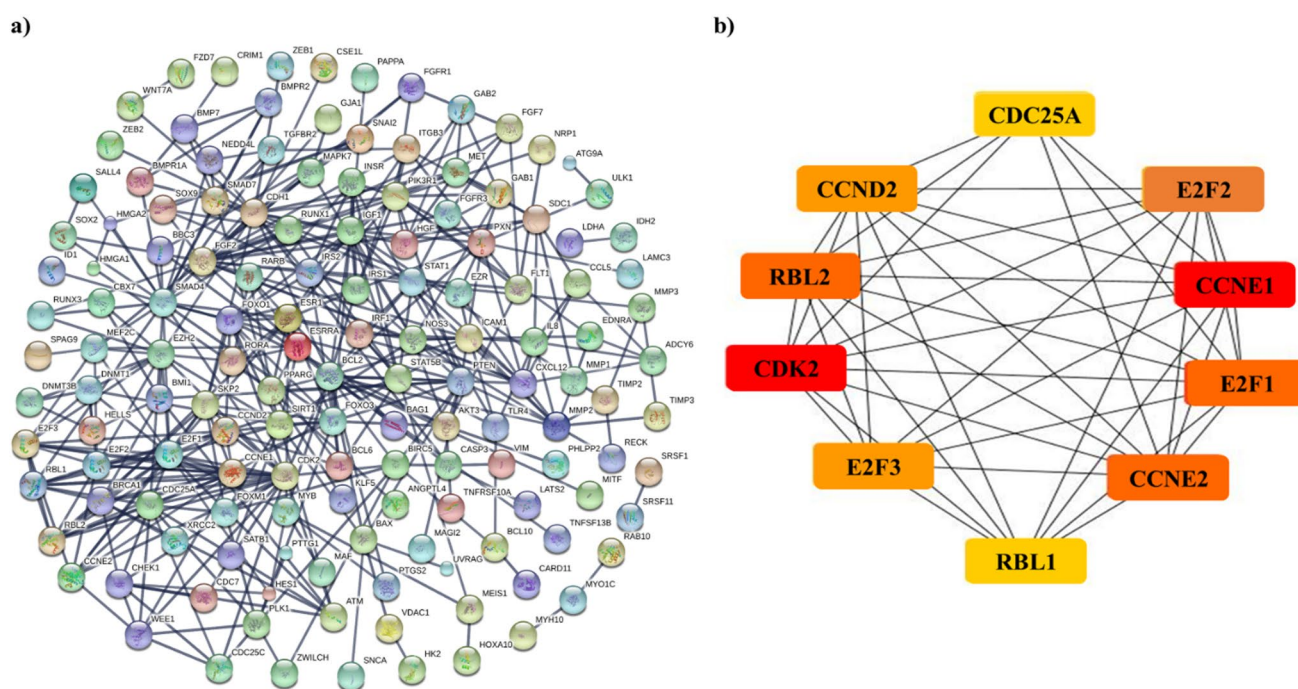


Fig. 4 Protein–protein interaction analysis and Hub gene detection. **a** PPIN was constructed by including all the 217 DEGs targets of the differentially expressed MCs via the STRING (V12.0) webserver. **b** The top 10 hub genes of PPIN were identified via the cytoHubba (V0.1) plugin. The PPIN and hub gene networks were visualized via the Cytoscape (v3.6.1) program. The 10 hub genes identified in the present study are *CDC25A*, *CCND1*, *CCNE1*, *CCNE2*, *E2F1*, *E2F2*, *E2F3*, *CDK2*, *RBL1*, *RBL2*, and *CDK2*

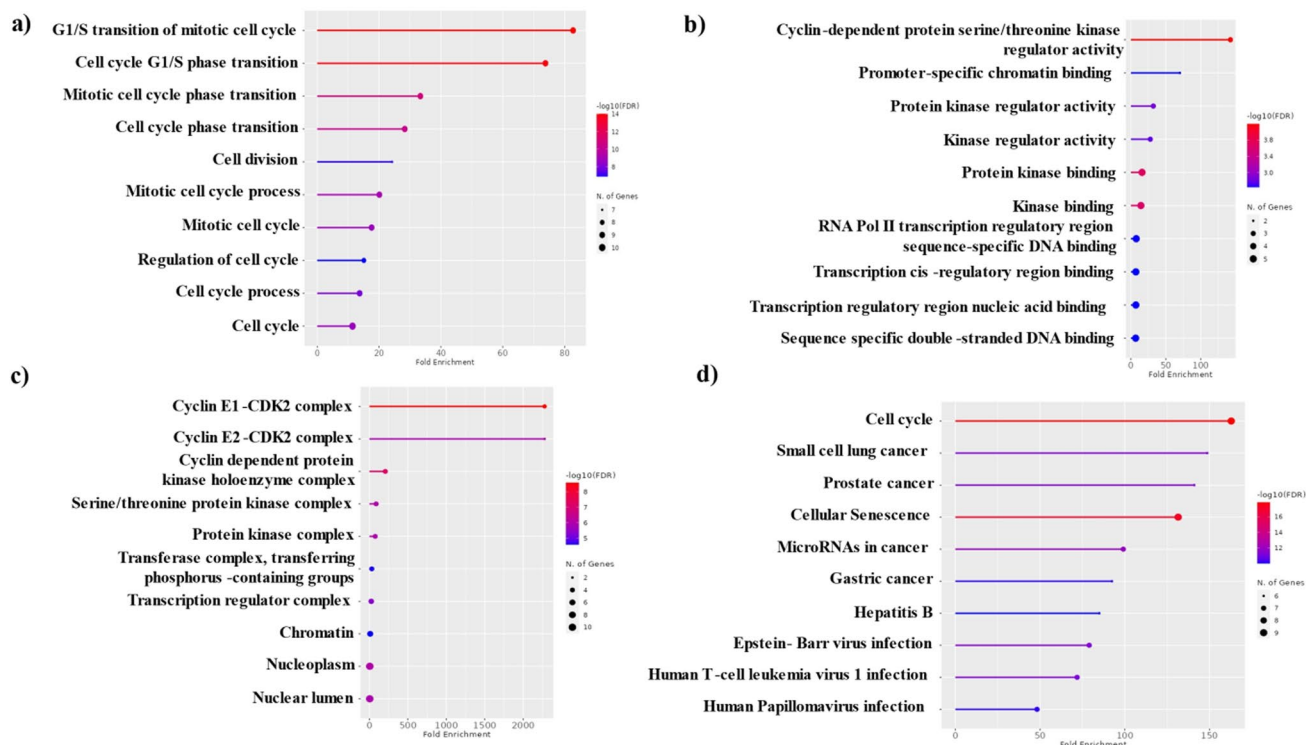


Fig. 5 Functional and pathway enrichment analysis of the top 10 Hub genes. **a** to **d** The top ranked biological processes, cellular components, molecular functions and KEGG pathways enriched according to ShinyGO (V 0.80) analysis

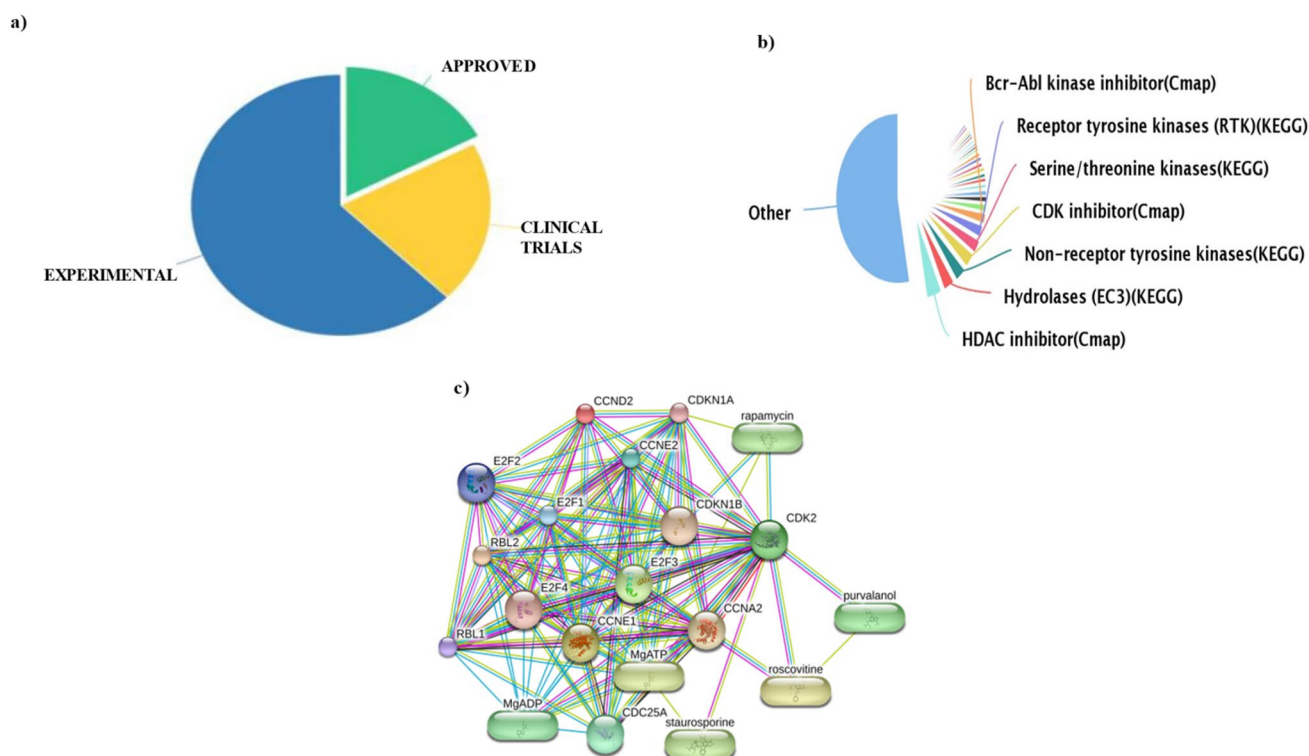


Fig. 6 Analysis of the associations of the hub genes with drugs. **a** Pie chart representing the drug approval status. We identified 28 approved drugs and 31 drugs in clinical trials that target MC cluster hub genes. Our analysis suggested that hub genes can be targeted by several drugs that are either approved or under clinical trials. **b** Pie chart representing the family of drugs that can target the hub genes. **c** Chemical and hub gene network generated from STITCH (V 5.0)

goal, we tested the prognostic potential by generating prognostic models by combining the random forest algorithm with miRNA cluster expression. Prognostic analysis with the TCGA-CESC dataset revealed 22 miRNAs linked to patient survival, and further analysis revealed that altered miRNA expression was correlated with metastasis in CC [40–42]. Thus, our analysis identified miRNA clusters with prognostic utility in CC. However, further studies are needed to confirm our findings.

One of the key findings of this study is the downregulation of the miR-379/656 cluster, which is commonly known as the chromosome 14 miRNA cluster. miR-379/656 is the second largest human miRNA cluster located at chromosome 14 in humans [43, 44]. Upregulation [45] and downregulation of this cluster have been reported in cancers [31, 44, 46, 47]. The members of this miRNA cluster are reported to be downregulated in CC. We selected four miRNAs from the miR-379/656 cluster (miR-376c, miR-409, miR-494, and miR-495) for validation in an independent cohort of NCE and CESC samples, as this cluster downregulation was observed in all four independent CC datasets analysed. miR-376c is one of the downregulated miRNA clusters in CC. miR-376c targets BMI1 (B-cell-specific Moloney murine leukemia virus integration site 1) to inhibit proliferation, G1/S phase transition, and invasion [48]. miR-409-3p is a downregulated miRNA in CC. Another study revealed that miR-409-3p is downregulated and has an inverse correlation with HPV E6 in CC. Thus, the downregulation of host miRNAs that target HPV oncogenes may be critical during CC [49]. Reactivation of miR-409-3p hindered the growth and motility of CC cells by directly targeting cyclin-dependent kinase 8 (CDK8) [50]. Downregulation of miR-409-3p impacts the overall survival of CC patients and is inversely correlated with AKT [51]. Significantly lower expression of miR-494 was reported in CC tissues than in normal and cervical intraepithelial neoplasia samples. Compared with control cells, HeLa cells transfected with miR-494 mimics presented reduced proliferation and invasion rates [52]. Another study revealed the upregulation of miR-494 with concomitant downregulation of phosphatase and TENsin homologue (PTEN) in CC [53]. A correlation between miR-494 overexpression and poor overall survival and poor prognosis has also been reported. Furthermore, increased plasma miR-494 levels correlated with the degree of cancer invasion in CC. The study also demonstrated that the induction of proliferation, migration, and invasion upon miR-494 overexpression involves activation of the MAPK/ERK pathway via direct targeting of SOX9 [54]. The study did not mention the possible mechanisms for the upregulated expression of miR-494. However, most of the previous studies, including

ours, reported the downregulation of miR-494 in CC [52, 55]. In addition, we noted a lower level of miR-494 in the TCGA-CESC dataset. Studies have shown that miR-494 is epigenetically regulated in cancers such as hepatocellular carcinoma [56], bladder cancer [57] and breast cancer [58]. miR-495-3p is another downregulated miRNA in CC. Ectopic coexpression of miR-495-3p and miR-143-3p inhibited CC cell viability by promoting apoptosis, inhibited tumor growth in vivo and targeted Cyclin Dependent Kinase 1 (CDK1) in CC [59]. The improperly expressed miRNA clusters identified in our investigation may function as biomarkers for CC. Studies have described both the upregulation and downregulation of miR-494 in CC. Our findings are consistent with those of most previous studies showing that miR-494 is downregulated and a tumor-suppressive miRNA in CC. Since these miRNAs are differentially expressed, their use as biomarkers for CC is promising. However, detailed mechanistic studies are needed to fully understand the role of the miR-379/656 cluster in CC.

Functional enrichment analysis of miRNA cluster targets revealed the involvement of key pathways, such as PI3K–Akt signalling and p53 signalling, which are critical in CC progression [60]. GO analysis highlighted enriched processes such as epithelial cell proliferation, reproductive system development, and cell cycle regulation, suggesting that aberrant miRNA cluster expression may promote CC aggressiveness. These pathways are closely linked to oncogenic transformation and tumor progression. We constructed a protein–protein interaction network (PPIN) of miRNA cluster targets, identifying hub genes such as *CDC25A*, *CCNE1*, *E2F1*, *CCNE2*, *RBL1*, *E2F3*, *CDK2*, *RBL2*, *E2F2* and *CCND2*, which are crucial in cell cycle regulation, cellular senescence, and cancer-related pathways [61]. Thus, targeting these miRNA clusters may benefit CC management.

Nevertheless, our study has several limitations. First, the number of clinical samples used in the current study was small. Second, we did not perform any mechanistic studies to understand the molecular mechanisms and signalling pathways contributing to CC. The bias due to the small sample size was overcome by analysing publicly available datasets from CC and validation studies using independent samples by qRT–PCR. We detected concordance between the small RNA sequencing data and the qRT–PCR data. We used a standardized pipeline for data analysis and considered genes as differentially expressed if LogFC (log2fold change) > +1 and < –1 with an FDR of < 0.05. Furthermore, we used differentially expressed genes from each dataset for comparison to avoid errors due to the use of different platforms. Our findings identified several novel miRNA clusters whose functions in CC pathology have yet to be established. Although promising, the study findings require validation in a larger sample size and necessitate mechanistic studies to understand their function in CC. We plan to validate the expression of miRNAs in a large cohort of samples and characterize their functions via in vitro and in vivo studies as part of future research.

5 Conclusion

In conclusion, our study identified miRNA clusters whose targets are altered in CC. We identified 48 significantly differentially expressed miRNA clusters and 22 prognostically important miRNAs. Interestingly, we identified and confirmed the downregulation of the miR-379/656 cluster in CC. This study identified several key cancer-related pathways, notably the p53 pathway, the cell cycle, and MAPK signalling. Target gene analysis identified *CDC25A*, *CCNE1*, *E2F1*, *CCNE2*, *RBL1*, *E2F3*, *CDK2*, *RBL2*, *E2F2* and *CCND2* as the top ten MC target hub genes. Future research should involve larger cohorts and experimental studies to validate the roles of identified miRNA clusters in CC. Overall, we identified the aberrant expression of miRNA clusters relevant to CC. The targeting of these clusters may be attempted to manage CC.

Acknowledgements We thank the Science and Engineering Research Board (SERB), Department of Science and Technology (DST), Government of India (Grant No: EMR/2016/002314 and Grant No: MTR/2021/000182), SPARC grant (SPARC/2019-2020/P2297/SL) and DBT/Wellcome Trust India Alliance Intermediate Fellowship (Grant No. IA/I/22/1/506240) for funding the study. We acknowledge Dr. TMA Pai Structured Ph.D. fellowship program at MAHE for fellowship and DBT/Wellcome Trust India Alliance Intermediate Fellowship (Grant No. IA/I/22/1/506240) awarded to Shama Prasada Kabekkodu. The authors also thank the Manipal Academy of Higher Education, Manipal, Technology Information Forecasting and Assessment Council (TIFAC) Core in Pharmacogenomics at MAHE, the Manipal, the Fund for Improvement of S&T Infrastructure (FIST), the Karnataka Fund for Infrastructure Strengthening in Science and Technology (K-FIST), the Government of Karnataka, and the Builder Grant, Department of Biotechnology, Government of India.

Author contributions SHK, PVJ, VKV, VS performed the experiment, analysis, writing SM, SC, SPK supervised and corrected the manuscript KS, DK provided clinical inputs.

Funding We thank the Science and Engineering Research Board (SERB), Department of Science and Technology (DST), Government of India (Grant No: EMR/2016/002314 and Grant No: MTR/2021/000182), Ministry of Human Resource Development (Grant No: SPARC/2019–2020/P2297/SL) and DBT/Wellcome Trust India Alliance Intermediate Fellowship (Grant No. IA/I/22/1/506240) for funding the study.

Data availability All data underlying the results are available as part of the article and no additional source data are required.

Declarations

Competing interests The authors declare no competing interests.

Open Access This article is licensed under a Creative Commons Attribution-NonCommercial-NoDerivatives 4.0 International License, which permits any non-commercial use, sharing, distribution and reproduction in any medium or format, as long as you give appropriate credit to the original author(s) and the source, provide a link to the Creative Commons licence, and indicate if you modified the licensed material. You do not have permission under this licence to share adapted material derived from this article or parts of it. The images or other third party material in this article are included in the article's Creative Commons licence, unless indicated otherwise in a credit line to the material. If material is not included in the article's Creative Commons licence and your intended use is not permitted by statutory regulation or exceeds the permitted use, you will need to obtain permission directly from the copyright holder. To view a copy of this licence, visit <http://creativecommons.org/licenses/by-nc-nd/4.0/>.

References

1. Sung H, Ferlay J, Siegel RL, et al. Global Cancer Statistics 2020: GLOBOCAN estimates of incidence and mortality worldwide for 36 cancers in 185 countries. *CA Cancer J Clin*. 2021;71:209–49.
2. Arbyn M, Weiderpass E, Bruni L, et al. Estimates of incidence and mortality of cervical cancer in 2018: a worldwide analysis. *Lancet Glob Health*. 2020;8:e191–203.
3. Singh M, Jha RP, Shri N, et al. Secular trends in incidence and mortality of cervical cancer in India and its states, 1990–2019: data from the Global Burden of Disease 2019 Study. *BMC Cancer*. 2022;22:149–149.
4. Lin M, Ye M, Zhou J, et al. Recent advances on the molecular mechanism of cervical carcinogenesis based on systems biology technologies. *Comput Struct Biotechnol J*. 2019;17:241–50.
5. Koliopoulos G, Nyaga VN, Santesso N, et al. Cytology versus HPV testing for cervical cancer screening in the general population. *Cochrane Database Syst Rev*. 2017. <https://doi.org/10.1002/14651858.CD008587.pub2>.
6. He Z, Chen R, Hu S, et al. The value of HPV genotypes combined with clinical indicators in the classification of cervical squamous cell carcinoma and adenocarcinoma. *BMC Cancer*. 2022;22:776–776.
7. Macios A, Nowakowski A. False negative results in cervical cancer screening—risks, reasons and implications for clinical practice and public health. *Diagnostics*. 2022;12:1508–1508.
8. Li J, Zhang X, Wang P, et al. The help of HPV integration testing to avoid the misdiagnosis of a patient with stage ia1 cervical cancer: a case report and literature review. *Pharmacogenom Pers Med*. 2021;14:1457–61.
9. Mremi A, Mchome B, Mlay J, et al. Performance of HPV testing, Pap smear and VIA in women attending cervical cancer screening in Kilimanjaro region, Northern Tanzania: a cross-sectional study nested in a cohort. *BMJ Open*. 2022;12:e064321–e064321.
10. Cancer Genome Atlas Research Network, Albert Einstein College of Medicine, Analytical Biological Services, et al. Integrated genomic and molecular characterization of cervical cancer. *Nature*. 2017;543:378–84.
11. Varghese VK, Shukla V, Jishnu PV, et al. Characterizing methylation regulated miRNA in carcinoma of the human uterine cervix. *Life Sci*. 2019;232:116668–116668.
12. Shukla V, Varghese VK, Kabekkodu SP, et al. Enumeration of deregulated miRNAs in liquid and tissue biopsies of cervical cancer. *Gynecol Oncol*. 2019;155:135–43.
13. Kabekkodu SP, Shukla V, Varghese VK, et al. Clustered miRNAs and their role in biological functions and diseases. *Biol Rev*. 2018;93:1955–86.
14. Kozomara A, Birgaoanu M, Griffiths-Jones S. miRBase: from microRNA sequences to function. *Nucleic Acids Res*. 2019;47:D155–62.
15. Wang Y, Luo J, Zhang H, et al. microRNAs in the same clusters evolve to coordinately regulate functionally related genes. *Mol Biol Evol*. 2016;33:2232–47.
16. Kabekkodu SP, Bhat S, Pandey D, et al. Prevalence of human papillomavirus types and phylogenetic analysis of HPV-16 L1 variants from Southern India. *Asian Pac J Cancer Prev APJCP*. 2015;16:2073–80.
17. Sun Z, Evans J, Bhagwate A, et al. CAP-miRSeq: a comprehensive analysis pipeline for microRNA sequencing data. *BMC Genomics*. 2014;15:423–423.
18. Chan W-C, Ho M-R, Li S-C, et al. MetaMirClust: discovery of miRNA cluster patterns using a data-mining approach. *Genomics*. 2012;100:141–8.
19. Huang H-Y, Lin Y-C-D, Li J, et al. miRTarBase 2020: updates to the experimentally validated microRNA–target interaction database. *Nucleic Acids Res*. 2020. <https://doi.org/10.1093/nar/gkz896>.
20. McGeary SE, Lin KS, Shi CY, et al. The biochemical basis of microRNA targeting efficacy. *Science*. 2019. <https://doi.org/10.1126/science.aav1741>.
21. Hauschild A-C, Pastrello C, Ekaputeri GKA, et al. MirDIP 5.2: tissue context annotation and novel microRNA curation. *Nucleic Acids Res*. 2023;51:D217–25.
22. Ge SX, Jung D, Yao R. ShinyGO: a graphical gene-set enrichment tool for animals and plants. *Bioinformatics*. 2020;36:2628–9.
23. Szklarczyk D, Gable AL, Lyon D, et al. STRING v11: protein–protein association networks with increased coverage, supporting functional discovery in genome-wide experimental datasets. *Nucleic Acids Res*. 2019;47:D607–13.
24. Chin C-H, Chen S-H, Wu H-H, et al. cytoHubba: identifying hub objects and subnetworks from complex interactome. *BMC Syst Biol*. 2014;8:S11–S11.
25. Otasek D, Morris JH, Bouças J, et al. Cytoscape automation: empowering workflow-based network analysis. *Genome Biol*. 2019;20:185–185.
26. Chou P-H, Liao W-C, Tsai K-W, et al. TACCO, a database connecting transcriptome alterations, pathway alterations and clinical outcomes in cancers. *Sci Rep*. 2019;9:3877–3877.

27. Piñeiro-Yáñez E, Reboiro-Jato M, Gómez-López G, et al. PanDrugs: a novel method to prioritize anticancer drug treatments according to individual genomic data. *Genome Med.* 2018;10:41.
28. Xu F, Wang Y, Ling Y, et al. dbDEMC 3.0: functional exploration of differentially expressed miRNAs in cancers of human and model organisms. *Genomics Proteom Bioinform.* 2022;20:446–54.
29. Wilting SM, Snijders PJF, Verlaet W, et al. Altered microRNA expression associated with chromosomal changes contributes to cervical carcinogenesis. *Oncogene.* 2013;32:106–16.
30. Gao D, Zhang Y, Zhu M, et al. miRNA expression profiles of HPV-infected patients with cervical cancer in the Uyghur population in China. *PLoS ONE.* 2016;11: e0164701.
31. Srinath S, Jishnu PV, Varghese VK, et al. Regulation and tumor-suppressive function of the miR-379/miR-656 (C14MC) cluster in cervical cancer. *Mol Oncol.* 2024;18:1608–30.
32. Backes C, Khaleeq QT, Meese E, et al. miEAA: microRNA enrichment analysis and annotation. *Nucleic Acids Res.* 2016;44:W110–6.
33. Chang L, Zhou G, Soufan O, et al. miRNet 2.0: network-based visual analytics for miRNA functional analysis and systems biology. *Nucleic Acids Res.* 2020;48:W244–51.
34. Tang G, Cho M, Wang X. OncoDB: an interactive online database for analysis of gene expression and viral infection in cancer. *Nucleic Acids Res.* 2022;50:D1334–9.
35. Kuhn M, von Mering C, Campillos M, et al. STITCH: Interaction networks of chemicals and proteins. *Nucleic Acids Res.* 2008;36:684–8.
36. Catarino R. Cervical cancer screening in developing countries at a crossroad: emerging technologies and policy choices. *World J Clin Oncol.* 2015;6:281–281.
37. Condrat CE, Thompson DC, Barbu MG, et al. miRNAs as biomarkers in disease: latest findings regarding their role in diagnosis and prognosis. *Cells.* 2020;9:276–276.
38. Wang J, Chen L. The role of miRNAs in the invasion and metastasis of cervical cancer. 2019. *Biosci Rep.* <https://doi.org/10.1042/BSR20181377>.
39. Gómez-Gómez Y, Organista-Nava J, Gariglio P. Deregulation of the miRNAs expression in cervical cancer: human papillomavirus implications. *BioMed Res Int.* 2013;2013:1–15.
40. Adiga D, Eswaran S, Pandey D, et al. Molecular landscape of recurrent cervical cancer. *Crit Rev Oncol Hematol.* 2021;157:103178–103178.
41. Nalejska E, Mączyńska E, Lewandowska MA. Prognostic and predictive biomarkers: tools in personalized oncology. *Mol Diagn Ther.* 2014;18:273–84.
42. Bhandari V, Kausar M, Naik A, et al. Unusual metastasis from carcinoma cervix. *J Obstet Gynaecol India.* 2016;66:358–358.
43. Benetatos L, Hatzimichael E, Londin E, et al. The microRNAs within the DLK1-DIO3 genomic region: involvement in disease pathogenesis. *Cell Mol Life Sci.* 2013;70:795–814.
44. Laddha SV, Nayak S, Paul D, et al. Genome-wide analysis reveals downregulation of miR-379/miR-656 cluster in human cancers. *Biol Direct.* 2013;8:10.
45. Molina-Pinelo S, Salinas A, Moreno-Mata N, et al. Impact of DLK1-DIO3 imprinted cluster hypomethylation in smoker patients with lung cancer. *Oncotarget.* 2018;9:4395–410.
46. Kumar A, Nayak S, Pathak P, et al. Identification of miR-379/miR-656 (C14MC) cluster downregulation and associated epigenetic and transcription regulatory mechanism in oligodendrogliomas. *J Neurooncol.* 2018;139:23–31.
47. Kaur K, Kakkar A, Kumar A, et al. Clinicopathological characteristics, molecular subgrouping, and expression of miR-379/miR-656 cluster (C14MC) in adult medulloblastomas. *J Neurooncol.* 2016;130:423–30.
48. Deng Y, Xiong Y, Liu Y. miR-376c inhibits cervical cancer cell proliferation and invasion by targeting BMI1. *Int J Exp Pathol.* 2016;97:257–65.
49. Sommerova L, Anton M, Bouchalova P, et al. The role of miR-409-3p in regulation of HPV16/18-E6 mRNA in human cervical high-grade squamous intraepithelial lesions. *Antiviral Res.* 2019;163:185–92.
50. Zhou B, Li T, Xie R, et al. CircFAT1 facilitates cervical cancer malignant progression by regulating ERK1/2 and p38 MAPK pathway through miR-409-3p/CDK8 axis. *Drug Dev Res.* 2021;82:1131–43.
51. Li B, Wu N, Zhang X-J, et al. MicroRNA-409 inhibits the proliferative ability of cervical carcinoma cells by regulating AKT. *Eur Rev Med Pharmacol Sci.* 2018;22:936–42.
52. Cheng L, Kong B, Zhao Y, et al. miR-494 inhibits cervical cancer cell proliferation through upregulation of SOCS6 expression. *Oncol Lett.* 2017. <https://doi.org/10.3892/ol.2017.7651>.
53. Yang Y-K, Xi W-Y, Xi R-X, et al. MicroRNA-494 promotes cervical cancer proliferation through the regulation of PTEN. *Oncol Rep.* 2015;33:2393–401.
54. Yu N, Jin J, Liu J, et al. Upregulation of miR-494 promotes cervical cancer cell proliferation, migration and invasion via the MAPK/ERK pathway. *Int J Clin Exp Pathol.* 2017;10:3101–8.
55. Wen N, Zhang J, Zhang Q. MiR-494 inhibits the proliferation, migration and invasion of cervical cancer cells by regulating LETMD1. *Cell Mol Biol.* 2022;67:81–7.
56. Bergamini C, Leoni I, Rizzardi N, et al. MiR-494 induces metabolic changes through G6pc targeting and modulates sorafenib response in hepatocellular carcinoma. *J Exp Clin Cancer Res.* 2023;42:145–145.
57. Tian Z, Luo Y, Zhu J, et al. Transcriptionally elevation of miR-494 by new ChIA-F compound via a HuR/JunB axis inhibits human bladder cancer cell invasion. *Biochim Biophys Acta BBA - Gene Regul Mech.* 2019;1862:822–33.
58. Zhan M-N, Yu X-T, Tang J, et al. MicroRNA-494 inhibits breast cancer progression by directly targeting PAK1. *Cell Death Dis.* 2017;8:e2529–e2529.
59. Tang J, Pan H, Wang W, et al. MiR-495-3p and miR-143-3p cotarget CDK1 to inhibit the development of cervical cancer. *Clin Transl Oncol.* 2021;23:2323–34.
60. Kabekkodu SP, Shukla V, Varghese VK, et al. Cluster miRNAs and cancer: diagnostic, prognostic and therapeutic opportunities. *WIREs RNA.* 2020. <https://doi.org/10.1002/wrna.1563>.
61. Balasubramaniam SD, Balakrishnan V, Oon CE, et al. Key molecular events in cervical cancer development. *Medicina (Mex).* 2019;55:384–384.